

# **COMPARISON OF SEISMIC PERFORMANCE OF BASE-ISOLATED HOUSE WITH VARIOUS DEVICES**

SHINJI NAKATA<sup>1)</sup> TSUTOMU HANAI<sup>2)</sup> SHIN-ICHI KIRIYAMA<sup>1)</sup> and NOBUO FUKUWA<sup>3)</sup>

<sup>1)</sup> Asahi Kasei Homes Co., TOKYO 160-8345, Japan

Email: nakata.sb@om.asahi-kasei.co.jp

<sup>2)</sup> Nihon System Sekkei., TOKYO 103-0013, Japan

Email: hanai@nittem.co.jp

<sup>3)</sup> Department of Environmental Engineering and Architecture,

Nagoya University, Nagoya 464-8603, Japan

Email: fukuwa@sharaku.nuac.nagoya-u.ac.jp

## **ABSTRACT**

Recently, various base-isolated devices corresponding to the low-rised house have been developed in practical use. However, the common information for designers to select specific device has not gathered. Therefore, a full scale vibration test was conducted to grasp the difference of the isolated response by replacing only base-isolated devices system using common superstructure on the shaking table in which three directional simultaneous vibrations was possible. The base-isolated system used for this test was 2 kinds of ball bearing type and one slide type, which had been used for actual base-isolated houses. The result of the test tells that each devices system fulfills the basic performance demanded for base-isolated houses; response acceleration was reduced to input acceleration, and damage on superstructure was not found. Each devices system is evaluated from the point of response of each input wave, influence of vertical simultaneous vibration.

## **INTRODUCTION**

Various base isolation devices corresponding to the low-rised house have been developed and put into practical use since the Hyogoken Nanbu Earthquake of 1995, and ball-bearing type and slide type base isolation devices have become widely used for wooden and steel-framed structures. Iba et al (1) conducted shaking table tests of a number of base isolation devices supporting weights. Response behavior of full-scale buildings, however, equipped with different base isolation devices (including devices and systems; the same applies hereafter) that have been put into practical use thus far have not yet been compared and verified under the same conditions. At present, designers are not given information that would enable them to select appropriate base isolation devices according to such factors as the characteristics of input ground motions, building site restrictions, and the owner's preferences.

The authors therefore conducted a vibration test using a shaking table capable of simultaneous three-axis excitation. In the test, different base isolation devices were tested with the same superstructure placed on the shaking table in order to compare the responses obtained with the different base isolation devices. The base isolation devices used in the test were two types of ball-bearing devices and one type of sliding devices .

In the test, ground motions of near-field inland earthquakes and of interplate earthquakes containing long period components were used as input ground motions. Medium-level to close-to-2G horizontal excitation and simultaneous three-axis excitation involving more-than-1G vertical motions were conducted to investigate response changes due to different levels of input and the effects of vertical motion inputs on response. The test building was provided with finishing to observe damage due to superstructure response and with high-aspect-ratio furniture to determine the causes of furniture toppling.

The test results were examined to identify the characteristics of the responses obtained with different types of base isolation devices. And information useful for the performance-based design of base-isolated houses was extracted.

## **FULL SCALE VIBRATION TEST**

### Test building

The test building consisting of an isolated layer and a two-story superstructure was placed on a heavy-steel-frame foundation secured on a shaking table. Photo 1 and Figure 1 show the test setup, and Figure 2 shows the test building in plan view. The superstructure is a load-bearing-panel type, post-and-beam structure built with light steel framing. The plan dimensions of the first floor are 6.710 m by 6.405 m; the height of the first and second stories is 2.87 m; and the total weight of the house structure including the first-floor beams is about 302 kN.



Photo 1. Test setup

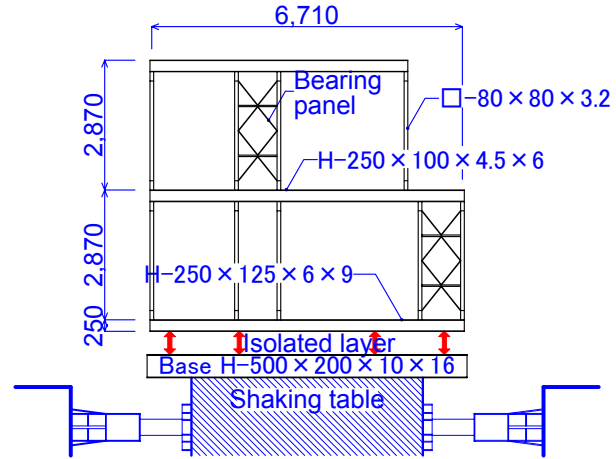


Fig.1. Test section

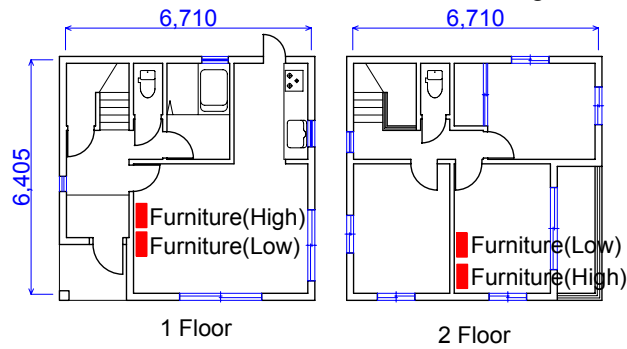


Fig.2. Test plan

### Isolated layer structure








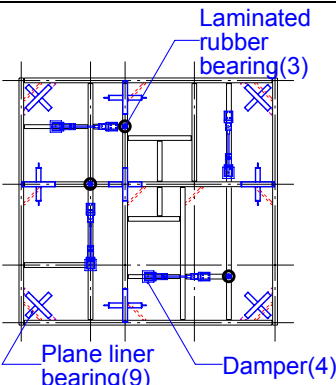
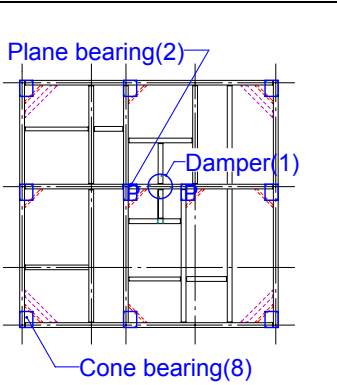
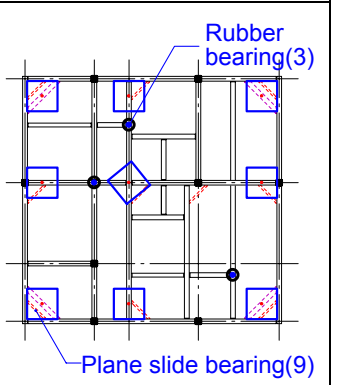
The three types of base isolation devices shown in Table 1 were used in the test. Type A device (system; the same applies hereafter) consists of ball-type plane linear bearings, laminated rubber bearings used as a source of restoring force, and viscous dampers. The laminated rubber bearings and dampers are located so that their contribution is evenly distributed. Type B device consists of ball-in-cone bearings located along the periphery of the isolated layer, and plane ball bearings with anti-torsion guides and viscous dampers located at the center of the isolated layer. The loose slope of the cone provides restoring force, and one characteristic of this mechanism is that there is no particular period of vibration. Type C device consists of plane slide bearings combined with non-laminated rubber bearings used as a source of restoring force. The non-laminated rubber bearings are located so that their contribution is evenly distributed. This damper less device is designed to consume energy by friction. Table 1 shows the factory-set characteristic values of each device. As shown, the coefficient of frictions  $\mu$  of the ball bearings and the slide bearings differ by a factor of 10 or so.

### Excitation and measurement methods

Excitation was performed using the three-dimensional shaking table at the Technical Research Institute of Obayashi Corporation. Table 2 shows the specifications of the shaking table including the horizontal and vertical excitation capability of the shaking table.

Figure 3 shows the locations of the measuring instruments used. Relative displacement between the isolated layer and the superstructure in the two horizontal directions was measured with a laser displacement meter (resolution: 0.01–0.05 mm, sampling time: 1/1,000 s). Building response was measured with strain-gauge accelerometers (effective range: 0.001G–5G).

Table1. Base isolation devices in the Test

TYPE	Type A	Type B	Type C
Bearing	 <p>Plane linear bearing  <math>\mu = 0.0033</math>  Limit <math>\delta = \pm 400\text{mm}</math></p>	 <p>Cone bearing   Plane bearing  <math>\mu = 0.006</math>  Limit <math>\delta = \pm 285\text{mm}</math></p>	 <p>Plane slide bearing  <math>\mu = 0.046</math>  Limit <math>\delta = \pm 350\text{mm}</math></p>
Restoring force	 <p>Laminated rubber bearing  <math>K = 38.5\text{N/mm}</math>  Limit <math>\delta = \pm 400\text{mm}</math></p>	<p>Slope</p>	 <p>Rubber bearing  <math>K = 31.2\text{N/mm}</math>  Limit <math>\delta = \pm 400\text{mm}</math></p>
Damping	 <p>Viscous damper  Damping force 17kN  Limit velocity 75cm/s  Limit <math>\delta = \pm 500\text{mm}</math></p>	 <p>Viscous damper  Damping force 12kN  Limit velocity 75cm/s  Limit <math>\delta = \pm 285\text{mm}</math></p>	—
Location			

Building response in the two horizontal directions was measured at the steel frame base, first floor, second floor and roof floor levels. Building response in the vertical direction was measured at the steel frame base, first floor and roof floor levels. The sampling frequency used for the measurement was 200 Hz.

### Input ground motions

As shown in Table 3, the following ground motions were used as inputs: ground motions of five historical earthquakes; simulated ground motions for three types of surface ground layer with different vibration periods,  $T_g$ , of elastic ground defined in accordance with the Ministry of Construction Notification No. 1457 for the response spectra of exposed engineering bedrock described in Article 82-6 of the Building Standard Law Enforcement Ordinance ("Notification waves  $y_{Sa}$ "); and medium intensity ground motions and harmonic sine waves used for confirming the initial motion.

Table2 Specification of the shaking table

	Horizontal	Vertical	Note
Acceleration maximum	3000cm/s <sup>2</sup>	1000cm/s <sup>2</sup>	Loading mass 50t Table size 5m×5m Shaking frequency DC~50Hz
Velocity maximum	200cm/s	100cm/s	
Displacement maximum	±60cm	±20cm	

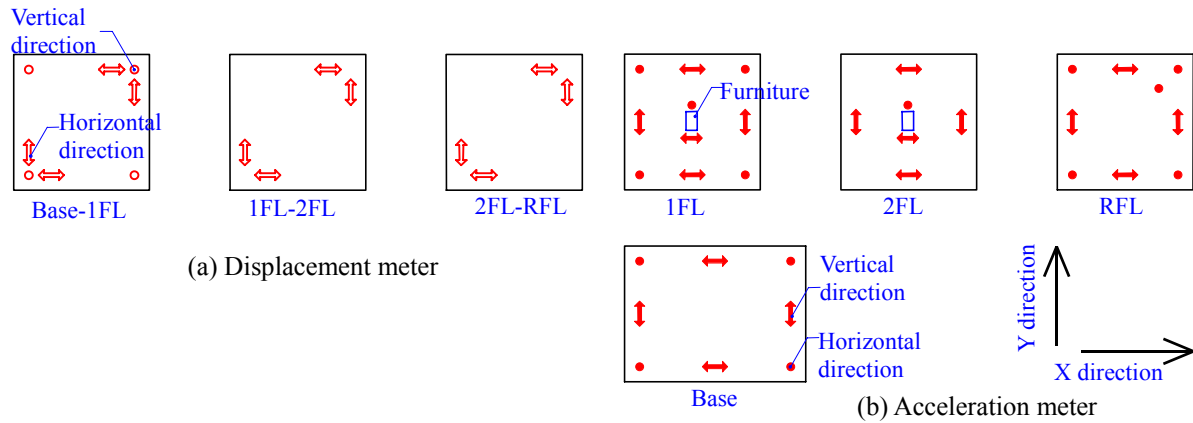


Fig.3 Location of measuring instrument

Figure 4 shows pseudo spectra of the Kobe, El Centro, Tarzana and Notification waves used as strong motion waves and of the medium intensity ground motion wave. The figure also shows response spectra at the steel frame base, but since a low cut filter was applied in order to protect the shaking table, the long-period components, particularly of the Notification waves, were lower than the target levels.

Excitation for the noncommented input waves was carried out to achieve the target level of 100%.

#### Characteristics of isolated layer and superstructure

Figure 5 shows the restoring force characteristics of the isolated layer achieved with different types of base isolation devices. Figure 5(a) also shows the load–deformation relationship in the case where sine wave excitation of the shaking table was continued for 20 seconds (hereafter referred to as "static excitation"), along with a nominal design value model. Figure 5(b) shows the load–deformation characteristics in the case where the superstructure was unfixed and dynamic excitation was applied to the isolated layer.

In the case of a Type A device, the nominal value is calculated by adding the Y-axis intercept loads for the ball bearings, laminated rubber bearings, and dampers. In static excitation, the load began to become larger than thenominal restoring force immediately after the initiation of rolling movement, and became about twice as large as the nominal value in the vicinity of the origin. One characteristic is that possibly because of the drum rotation mechanism, the dampers were made to carry a considerable amount of load from the stage at which the velocity was still as low as 1 to 2 cm/s (amplitude: 5 to 10 mm). In dynamic excitation, the contribution of the dampers became even greater because of velocity dependence, and the hysteresis loops were spindle-shaped.

Table3 The list of input ground motion

Input ground motions	$A_{\max}$	$V_{\max}$	$D_{\max}$	note
	(cm/s <sup>2</sup> )	(cm/s)	(cm)	
El Centro 1940 NS	486	50.0	13.7	Input level:50, 100%
Taft 1952 EW	529	50.0	22.7	
Hachinohe 1968 EW	266	50.0	14.7	
Kobe(JMA) 1995 NS	813	93.3	19.0	NS wave input X directions Input level:50~150%
〃 EW	619	81.3	15.7	
〃 UD	333	41.5	13.0	
Tarzana *1 NS	971	74.5	26.5	EW wave input X directions Input level:50~100%
〃 EW	1745	114.7	26.3	
〃 UD	1028	70.5	13.4	
Notification wavel (γSa 050)	490	65.6	28.6	Tg = 0.50 s
Notification wave 2 (γSa 075)	433	68.4	31.6	Tg = 0.75 s
Notification wave 3 (γSa 100)	364	68.8	35.8	Tg = 1.00 s
Taft phase				Input level:50~140%
Medium intensity ground motions*2	62~53	1.9~4.2	1.0~1.1	Shizuoka Prefecture 2001.4.3
Harmonic sine wave	Period 3s、Amplitude±10~±250mm			

\*1 Northridge 1994

\*2 Kyoshin Net (K-NET)

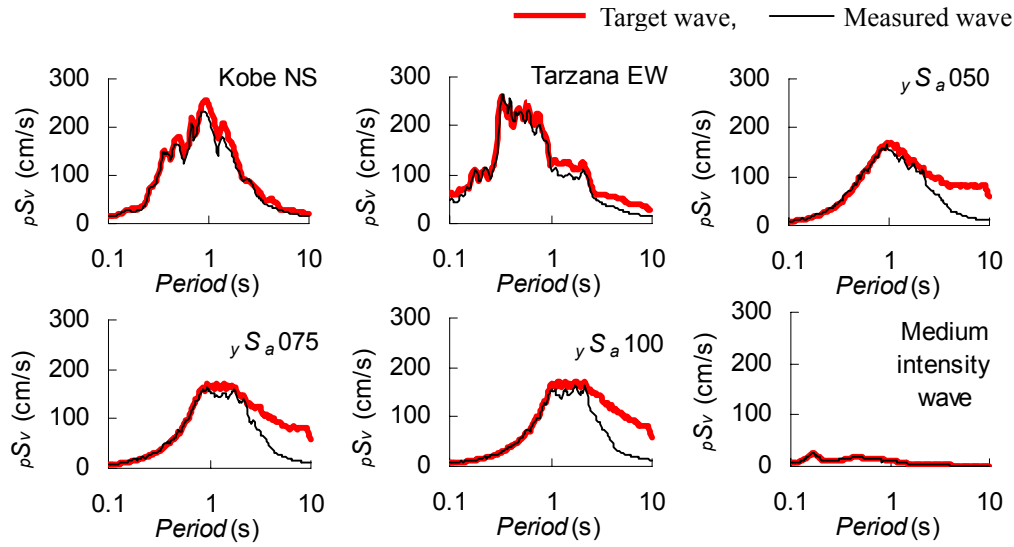
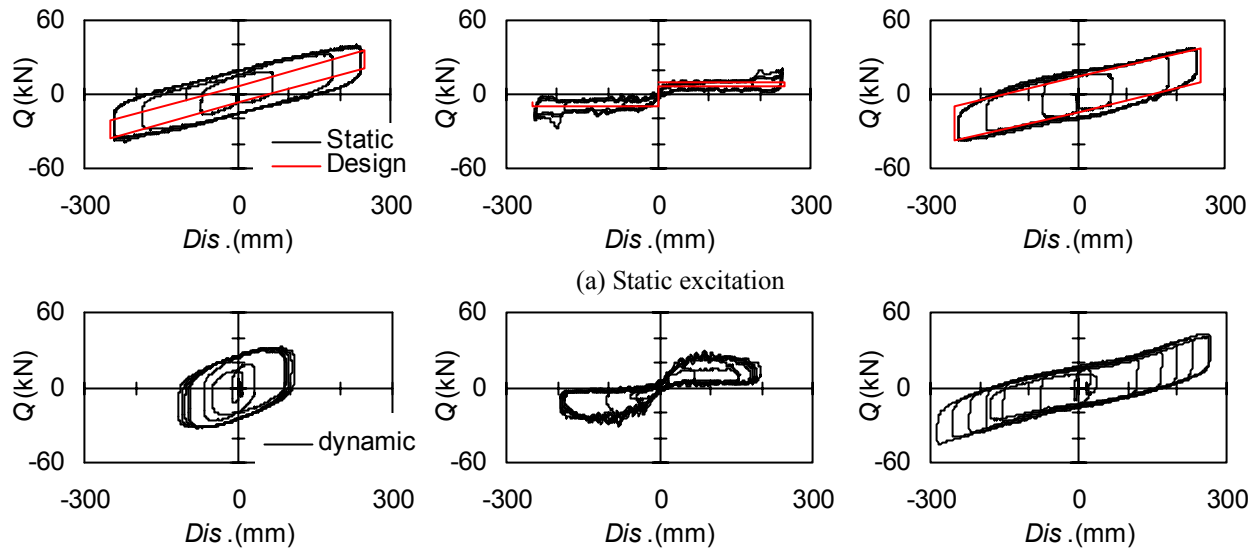


Fig.4. Pseudo velocity response spectra of the input target waves and the measured waves at the steel frame base

In the case of a Type B device, which includes the ball-in-cone bearings, the slope of the inner surface of the "cone" is constant and there is no natural period of vibration. Consequently, restoring force characteristics of this device are such that the resistance load varies only in the vicinity of the origin. The amount of load carried by the ball-type bearings is very small, and in the static loading, the amount of load carried by the dampers was not very large. In the dynamic loading, however, the amount of load carried by the dampers was large, and the restoring force characteristics observed can be described as viscous. The reason why little load was carried by the dampers in the vicinity of the origin where velocity was high is thought to be that the design of the device is such that the damper head is pressed against the upper surface.

In the case of a Type C device, the restoring force characteristics of the slide bearings and the nominal restoring force characteristics of the rubber bearings show close agreement in the static loading because there is no damper. More or less similar behavior was observed during the dynamic loading, indicating that velocity dependence is small.

The equivalent periods corresponding to a nominal displacement of 20 cm are 2.84 s for a Type A device, 3.71 s for a Type B device, and 2.73 s for a Type C device. The eccentricity ratio of the isolated layer is 0.01 for a Type A device, 0.03 for a Type B device, and 0.03 for a Type C device. During the three-second harmonic sine wave excitation in which considerable displacement occurred, little torsion was observed regardless of the type of



(b) Dynamic excitation (3-second harmonic sine wave excitation)

Fig.5. Restoring force characteristics of isolated layer

device used. As the characteristic of superstructure, the transfer functions between first floor and roof floor with the Kobe wave input shows the natural frequencies of superstructure is about 3Hz in the X and Y directions.

## TEST RESULTS

### Input level and maximum response value

In Figure 6, the horizontal axis shows the maximum value of the input velocity found by integrating the acceleration measured at the level of the steel frame base, and the vertical axis shows the maximum values of the response displacement of the isolated layer, the response shear coefficient at the level of each floor, and the response floor seismic intensity. "Floor seismic intensity" refers to a measured seismic intensity calculated by using the acceleration response waveform for each floor. Regardless of the type of device, the response displacement of the isolated layer was not greater than 250 mm, the response shear modulus for the first floor and the second floor was 0.22 or less and 0.26 or less, respectively, and the floor seismic intensity was not greater than "5 upper" on the Japan Meteorological Agency's seismic intensity scale. These results confirm the effectiveness of the base isolation devices.

In the case of a Type A device, the damping mechanism began to work when the velocity was still low, so the device was effective even against medium-level ground motions with an input velocity of 10 cm/s or less. The input velocity and the shear modulus show correlation. It can be said that characteristics of linearly behaving laminated rubber bearings and viscous damping are shown. In the cases of the other devices, there was a certain degree of response to medium-level ground motions, but the amount of response was relatively small even against strong ground motions. This indicates that climbing the slope of the ball-in-cone bearing (Type B device) and exceeding the sliding friction force requires a certain amount of input.

Isolated layer displacement tended to be minimized in the case where a Type A device was used and to be maximized in the case where a Type B device, which does not depend on displacement for restoring force, was used.

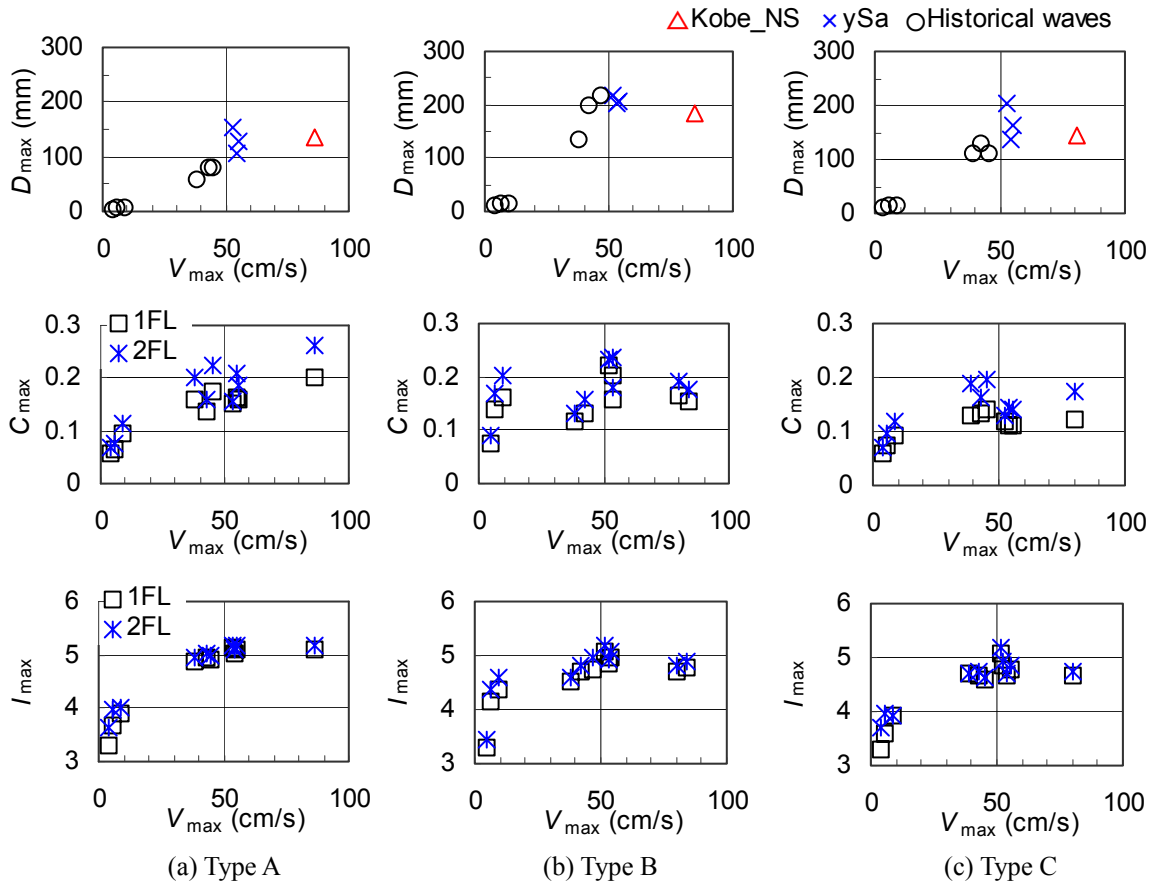


Fig.6. Relationship between input maximum velocity and response maximum value  
(Displacement of the isolated layer  $D_{\max}$ , Shear coefficient  $C_{\max}$ , Seismic intensity  $I_{\max}$ )

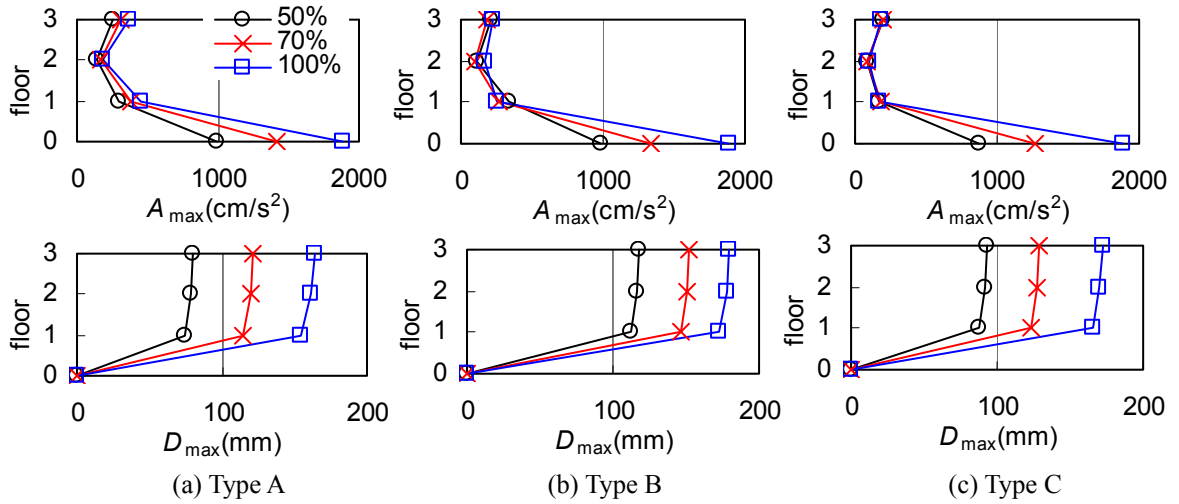


Fig.7. Relationship between input level of the Tarzana wave and maximum value  
(Acceleration  $A_{\max}$ , Displacement  $D_{\max}$ )

Let us now take a look at responses in the cases where input acceleration level is much greater than 1G. Figure 7 shows the maximum response acceleration and the maximum response displacement in the X direction in the cases where excitation was performed by varying the input level of the Tarzana wave along two horizontal axes between 50% and 100%.

Regardless of the type of device, the response acceleration was reduced to 1/3 to 1/6 of the input acceleration. Isolated layer displacement was within 25 cm, and the story drift angle of the first floor was not greater than 7 mm, indicating that there was no damage. No piece of furniture toppled over, either. Thus, all devices were effective against this type of input wave even against exceptionally high levels of input. The response acceleration of the superstructure did not show significant changes even when input acceleration was doubled. The amounts of change for a Type C device were particularly small. In the case of a Type A device, superstructure displacement somewhat increased as the input level rose. This response is thought to reflect the more or less linear nature of the stiffness of the isolated layer. The reason why greater response occurred in the case where a Type A device was used than in the cases where other devices were used is thought to be that the capacity of the viscous dampers was slightly too large for the weight of the overlying structure. However, effectiveness of base isolation is obvious even in the case of overdamping like this. As mentioned earlier, reduction of isolated layer displacement may be thought of as an advantage.

#### Effect of vertical motion

Let us take a look at the effects of vertical motion input. Figure 8 shows the load–deformation relationship for the isolated layer in the X direction in the cases of horizontal-two-axis excitation and three-axis excitation (maximum vertical acceleration:  $330 \text{ cm/s}^2$  and  $1,028 \text{ cm/s}^2$ ) using the Kobe and Tarzana waves. Compared with the two-axis excitation response, the three-axis excitation response hysteresis loops are characterized by small-scale load fluctuations. Isolated layer response displacements of the two ball-bearing type devices did not show significant differences, but the response displacements of the slide-bearing type device in the three-axis excitation were 6 to 9% smaller. Compared with the two-axis excitation, the response shear coefficient of the superstructure is considerably amplified, particularly with a Type B device subjected to the Kobe wave and with a Type B or Type C device subjected to the Tarzana waves whose vertical motion amplitude exceeds 1G. The maximum story drift angle of the superstructure, however, is only 1/442, which is well within the elastic range.

## CONCLUSIONS

The response properties of three types of base isolation devices have been compared under identical structural conditions and using identical input waves by conducting a shaking table test in which a single house superstructure was used in combination with different types of base isolation devices. All of the devices tested have proved effective so that for the input ground motions used in the test, the response acceleration was sufficiently lower than the input acceleration. No interior or exterior damage was found in the superstructure and bookcases placed in the structure did not topple over. Thus, it has been verified that the tested base isolation devices satisfy the basic performance requirements. The evaluation results are summarized below.



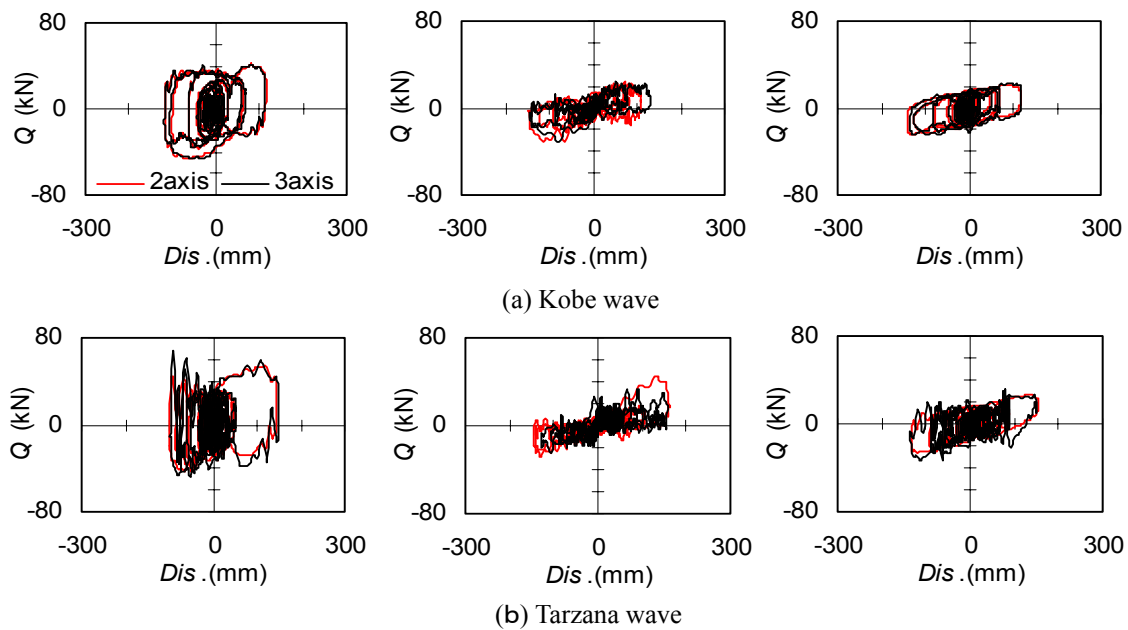


Fig.8. Influence of vertical motion on the load-deformation relationship for the isolated layer

1) Plane ball-bearing type device (Type A device): Since the capacity of the dampers used in the test was too large for the size of the building, the response acceleration of the building superstructure tended to be high. This tendency was particularly noticeable in the response to historical ground motions, but satisfactory results were obtained for long-period ground motions. It is believed that use of small dampers will expand the degrees of freedom in designing base-isolated houses.

2) Ball-in-cone bearing type device (Type B device): Devices of this type proved effective in reducing the response of the superstructure. In cases where the input level is high or the input ground motion contains a high percentage of long-period components, isolation layer displacement may reach the displacement limit of the device. It is therefore necessary either to increase damper capacity or to extend the displacement limit of the device.

3) Plane slide bearing type device (Type C device): The response of the superstructure to each ground motion was effectively reduced. Deformation tended to become large, however, in response to input waves dominated by long-period components. Incorporating viscous damping elements into slide type devices is thought to be a good way to improve the applicability of devices of this type to long-period motions or to reduce deformation.

4) Effects of vertical motion: Effects on shear force were observed in the case of 1G input in the vertical direction, but all base isolation devices proved effective against vertical motions.

Base isolation systems designed for single-family houses need to have the ability to stay still under short-return-period wind loads (trigger function) and the ability to resist fairly infrequent strong wind by the strength of the isolation layer although this was not verified in the test.

The authors are thinking of conducting follow-up studies on such considerations as how occupants feel when base isolation systems respond to wind loads, maintainability and durability of base isolation devices, and the total cost of base isolation systems. Such studies will facilitate the choice of base isolation devices that make effective use of their characteristics, and will also facilitate the design of base isolation systems, thereby making it possible to present performance options in designing base isolation system.

## REFERENCES

- Iiba, M., et al. (1999) "Three dimensional shaking table test on seismic behavior of isolators for houses Part1-6. In: Summaries of Technical Papers of Annual Meeting of Architectural Institute of Japan; Vol. B-2: 741-752 (in Japanese).
- Sakamoto, I., et al. (1999), "An experiment of base-isolated wooden house Part1-9. In: Summaries of Technical Papers of Annual Meeting of Architectural Institute of Japan; Vol. B-2: 715-732 (in Japanese).